# Resolution Limits in Lens-Integrated CMOS THz Cameras Employing Super-Resolution Imaging

Robin Zatta, Ritesh Jain, Janusz Grzyb, Ullrich R. Pfeiffer



2019 44th International Conference on Infrared, Millimeter, and Terahertz Waves (IRMMW-THz). https://doi.org/10.1109/IRMMW-THz.2019.8874510

---



---

# Resolution Limits in Lens-Integrated CMOS THz Cameras Employing Super-Resolution Imaging

Robin Zatta, Ritesh Jain, Janusz Grzyb, and Ullrich R. Pfeiffer
Institute for High-frequency and Communication Technology, University of Wuppertal, Germany
Email: zatta@uni-wuppertal.de

***Abstract*—In this paper, we discuss the design choices of CMOS THz cameras for achieving maximum angular resolution and high sensitivity over a large bandwidth. In an active THz imaging set-up, the spatial resolution becomes a function of the object magnification, determined by the focal length of the collimating optic and the camera's angular resolution. The THz camera investigated experimentally here, under-samples its field-of-view for incident frequencies above 0.578 THz due to its 80-µm pixel pitch coupled with narrow pixel beams. With the help of super-resolution imaging, the camera reaches a measured angular resolution of 1.92° at 0.652 THz. At 0.822 THz, where the camera exhibits optimum NEP, the presented super-resolution model predicts an estimated angular resolution of 1.7°.**

## I. Introduction

A camera consists of a focal plane array and an objective lens. Its angular resolution $\alpha$ determines the ability of a camera to distinguish between spatial details of an object. For a THz camera, diffraction presents a major physical constraint due to sub-millimeter wavelengths. Therefore, the angular resolution is influenced by various camera design and operation choices, such as number of pixels, pixel pitch, camera field-of-view (FoV), operation bandwidth, sensitivity, pixel directivity, and pixel isolation.

Associating radiation patterns of antenna-coupled THz camera pixels to the Rayleigh criterion, two pixels hit the angular resolution limit if the antenna beam pattern maximum of one pixel coincides with the first minimum of the other pixel [1]. Here, the dip between the two maxima of their combined antenna beam pattern is 26%. This optimum point is influenced by the antenna beam divergence angle $\varphi$ and the beam separation angle $\theta$. Unlike the beam divergence angle, the beam separation angle is a fixed design parameter obtained from the camera FoV divided by the number of pixels in one dimension. Below $f_o$, the pixel beams exhibit lower directivity, and this causes a larger beam overlap/smaller dip with image over-sampling. Above $f_o$, the pixel beams are too narrow, and the image is under-sampled. Therefore, super-resolution (SR) imaging used for over-sampling can further improve the angular resolution only above $f_o$ as indicated in Fig. 3. Fig. 1(a) illustrates the above-mentioned parameters, such as the beam separation angle, beam divergence angle, and the under-sampling issue. In Fig. 1(b), the Rayleigh criterion is shown based on two adjacent camera pixels.

In this work, we demonstrate the concept of SR imaging to improve upon the angular resolution of CMOS THz cameras and to analyze their resolution limits. Note that, unlike optical SR, which aims to transcend the physical diffraction limit [2], our experiment deals with geometrical SR, where the digital resolution for an under-sampled image gets enhanced towards the Rayleigh diffraction barrier [3].

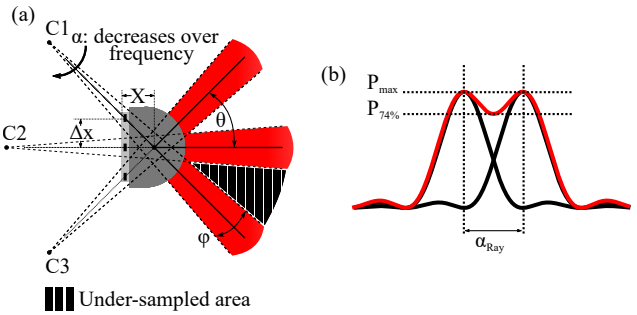


Figure 1. (a) Simplified geometrical model indicating the beam propagation of three adjacent camera pixels with virtual beam centers C1–C3 through the silicon lens. The pitch $\Delta x$ and the extension length X determine the beam separation angle $\theta$. The beam divergence angle $\varphi$ is inversely proportional to frequency. (b) Outlined individual beam patterns of two adjacent camera pixels and their combined pattern (red). The Rayleigh resolution limit $\alpha_{Ray}$ is reached if the dip between the two maxima is 26%.

## II. Experiment and Data Processing

The experimental set-up, shown in Fig. 2, was chosen to determine the angular resolution improvements and limitations of CMOS THz cameras by SR imaging. It comprises a 25-dBi 0.652-THz source, a CMOS THz camera [4], and an optical train. All components, except the source, were subsequently fixed within a cage system to ensure the stability of the optical alignment. This is crucial in avoiding any aberrations from mechanical raster-scanning. As illustrated in Fig. 2, the source beam is collected by a 50-mm PTFE-lens with an f-number of 2 to provide a collimated beam in the object plane for active THz imaging. After that, another 50-mm PTFE-lens with an f-number of 1, which matches the camera FoV of 46°, focusses the beam back onto the camera's silicon lens.

A metallic annular disc was raster-scanned in the xz-object plane within the optical train with a lateral/diagonal step size of 187.5/265.2 µm to sample at the sub-pixel level of the FPA. A total of 8x8 low-resolution (LR) images, each averaged over 1024 frames for a high sensitivity [5], were recorded and saved into an 8x8 matrix containing image information from 1024 pixels at 64 positions. The resulting imaging SNR and the total measurement time were 53 dB and 25 minutes, respectively.

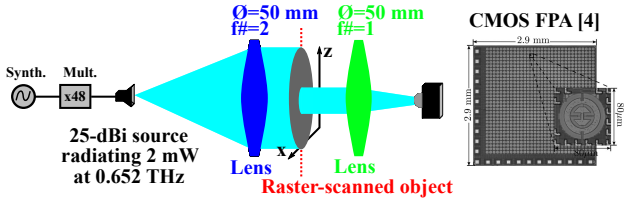


Figure 2. Experimental set-up and CMOS FPA. A metallic annular disc with a hole diameter of 15 mm has been raster-scanned with a lateral/diagonal step size of 187.5/265.2 µm within the optical train. Mechanical raster-scanning corresponds to sampling at the sub-pixel level of the FPA.

From this matrix, different SR images were super-composed in data processing. The notation for, e.g., the SR image composed of 3x3=9 LR images is '$SR_{9LR}$ image'. The mutual offsetting and superposition of LR images into a final SR image were realized through the SR algorithm from [6].

In the following, the edges in the diagonal of the LR/SR images are examined. Here, under-sampling is strongest due to $\sqrt{2}$ times larger center-to-center distance.

## III. Results

Fig. 3 compares the Rayleigh resolution limit across frequency to the measured results at 0.652 THz. The crossover frequency $f_o$ between over-sampling and under-sampling frequency regions and measured LR/SR images of a metallic annular disc are shown. The diagonal beam separation angle (blue) is calculated from the geometric relations between the lens and the sensor chip [7] with $\theta_{Diag}$=2.35°. The maximum achievable resolution $\alpha_{Ray}$ across frequency given by the Rayleigh limit (red) is calculated from the antenna aperture of the camera's 15-mm lens. Angular/spatial resolution for the LR/SR images are characterized from the edge response [8].

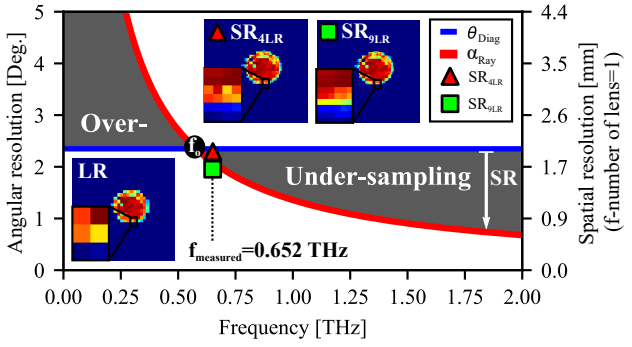


Figure 3. LR/SR images and their measured resolutions are compared to the Rayleigh resolution limit. Above $f_o$, SR imaging further improves the resolution. Over-sampling and under-sampling frequency regions are identified. The crossover frequency $f_o$ between such regions is 0.578 THz.

The calculated Rayleigh resolution at 0.652 THz is reached after super-composing 9 LR images, which demonstrates the proof of concept. Here, the measured angular resolution at 0.652 THz improved from $\alpha=\theta_{Diag}=2.35°$ to $\alpha=1.92°\approx\alpha_{Ray}$. For the chosen frame averaging at the camera readout of 1024, the estimated measurement time for the $SR_{9LR}$ image with an SNR of 53 dB was 3.5 minutes. Based on the experimental verification that the calculated Rayleigh resolution and the measured angular resolution approximately agree at 0.652 THz, the maximum angular resolution can be estimated over frequency by the SR model illustrated in Fig. 3. In this regard, the camera can reach an estimated angular resolution of 1.7° at 0.822 THz, where it exhibits optimum NEP.

In a 2-lens active THz imaging set-up, the collimating optic in front of the camera module translates the angular resolution into a spatial resolution. The spatial resolution thereby can be calculated as the product of angular resolution in radians and the focal length of the aforementioned optic, i.e., the spatial resolution becomes a function of object magnification. In our experiment, where the camera module is combined with a 50-mm PTFE-lens with an f-number of 1, the camera reaches a measured spatial resolution of 1.68 mm and an estimated spatial resolution of 1.48 mm (based on Rayleigh criterion) at 0.652 THz and 0.822 THz, respectively. In such 2-lens set-ups, the resolution further improves for narrower lens apertures.

## IV. Summary

In this paper, the resolution limits of a CMOS THz camera have been analyzed for the first time. The camera module under-samples above the optimum frequency $f_o$ due to its 80-µm pixel pitch coupled with narrow non-overlapping pixel beams. Note that every camera shows this behavior. Therefore, super-resolution imaging used for over-sampling can further improve the angular resolution only above $f_o$. In this regard, we have presented a super-resolution model that is capable of estimating the maximum achievable angular resolution across frequency given by the Rayleigh criterion. This model has been verified experimentally at 0.652 THz with a measured angular resolution of 1.92°. The super-resolution model, for example, predicts an estimated angular resolution of 1.7° at 0.822 THz, where the camera exhibits optimum NEP.

## Acknowledgements

The authors would like to thank Ticwave GmbH for providing the camera module. This work was partially funded by the DFG SFB/TRR 196 MARIE under project C08.

## References

[1] W. J. Smith, "Modern optical engineering," pp. 141–171, 2008.
[2] B. Huang *et al.*, "Breaking the diffraction barrier: super-resolution imaging of cells," *Cell*, vol. 143, no. 7, pp. 1047–1058, 2010.
[3] A. Borkowski *et al.*, "Geometrical superresolved imaging using nonperiodic spatial masking," *Journal of the Optical Society of America A*, vol. 26, no. 3, pp. 589–601, 2009.
[4] R. Al Hadi *et al.*, "A 1 k-pixel video camera for 0.7–1.1 terahertz imaging applications in 65-nm CMOS," *IEEE Journal of Solid-State Circuits*, vol. 47, no. 12, pp. 2999–3012, 2012.
[5] R. Zatta, R. Jain, and U. Pfeiffer, "Characterization of the noise behavior in lens-integrated CMOS terahertz video cameras," *Terahertz Sicience and Technology - The International Journal of THz*, vol. 11, no. 4, pp. 102–123, Dec. 2018.
[6] J. A. Kennedy *et al.*, "Improved image fusion in PET/CT using hybrid image reconstruction and super-resolution," *International journal of biomedical imaging*, vol. 2007, 2007.
[7] R. Jain, J. Grzyb, and U. R. Pfeiffer, "Terahertz light-field imaging," *IEEE Transactions on Terahertz Science and Technology*, vol. 6, no. 5, pp. 649–657, 2016.
[8] S. W. Smith *et al.*, "The scientist and engineer's guide to digital signal processing," *California Technical Pub. San Diego*, 1997.